Dynamics of ioninduceddipole capture: Effects of ion mass and collision energy

Lucia M. Babcock and Donald L. Thompson

Articles you may be interested in

Dynamic plasma screening effects on electron capture process in hydrogenic ion–fully stripped ion collisions in dense plasmas
Phys. Plasmas **4**, 2756 (1997); 10.1063/1.872144

The effect of the dipoleinduced dipole potential on ion–polar molecule collision rate constants
J. Chem. Phys. **96**, 5550 (1992); 10.1063/1.462695

Trajectory calculations of the effect of the induced dipole–induced dipole potential on ion–polar molecule collision rate constants
J. Chem. Phys. **85**, 3127 (1986); 10.1063/1.451023

Collisions in a noncentral field: A variational and trajectory investigation of ion–dipole capture
J. Chem. Phys. **72**, 2641 (1980); 10.1063/1.439409

Energy dependence of the differential cross sections for simple models of ioninduced dipole capture collisions
J. Chem. Phys. **71**, 1128 (1979); 10.1063/1.438457

Dynamics of ion-induced-dipole capture: Effects of ion mass and collision energy[a]

Lucia M. Babcock

Department of Chemistry, Louisiana State University, Baton Rouge, Louisiana 70803

Donald L. Thompson

Chemistry Division, University of California, Los Alamos National Laboratory and Department of Chemistry, Oklahoma State University, Stillwater, Oklahoma 74078[b]

Quasiclassical trajectories have been used to investigate ion–molecule complex formation and dissociation in model systems. A model ion-induced-dipole potential was used to represent the long-range attractive forces and an exponential was used for the repulsive part of the potential. The emphasis is on $Cl^- + Cl_2 \rightleftarrows [Cl_3^-]^*$, with some studies of the influence of ion mass on capture and lifetime. Capture cross sections as a function of complex lifetime were computed.

I. INTRODUCTION

We report here a quasiclassical trajectory study of complex formation in collisions between ions and a nonpolar molecule. Because of the long-range and purely attractive forces between an ion and a molecule, a feature of the collision dynamics is a process called capture wherein the pair attract each other and form a complex. *Capture* has long been a prominent concept in ion–molecule chemistry. Ion–molecule processes are often visualized as involving two steps: (1) capture, followed by (2) chemical reaction, electronic transition, collisional stabilization, or other events. Ion-induced-dipole capture is usually assumed to be described by the Langevin model.[1] This model is based on the idea that the ion-induced-dipole attractive force

$$V(R) = -q^2\alpha/2R^2 , \qquad (1)$$

leads to the formation of a complex, i.e., capture. [In Eq. (1), q is the charge on the ion and α is the polarizability of the molecule.] The Langevin capture cross section is

$$\sigma_2(E_{rel}) = \pi q (2\alpha/E_{rel})^{1/2} \qquad (2)$$

for relative translation energy E_{rel}. This expression is obtained by defining capture as those trajectories which cross the effective centrifugal barrier due to $L^2/2\mu R^2$, where L is the orbital angular momentum. Thus, the Langevin cross section includes all trajectories which encounter the inner wall of the ion–molecule potential at least once. It thus gives an upper limit for the cross section for complex formation. It generally predicts a capture rate coefficient on the order of 10^{-9} cm^3/molecules for small systems at room temperature.[2]

Classical trajectories can be, and have been, used to obtain an accurate description of the nature of ion–molecule capture collisions.[3–15] Dugan and co-workers[3–10] used trajectories to study ion–dipole collisions, for which they defined capture in much the same way as in the Langevin model. Chesnavich, Su, and Bowers[11,12] used a combined phase-space/trajectory approach[16] to investigate capture in ion-polar molecule systems. Hase and co-workers[13,14] have examined both capture and complexes in alkali ion–water molecule collisions. They define capture as those trajectories which experience more than one inner turning point in the ion–molecule relative motion.

We recently reported the results of a quasiclassical trajectory study of complex formation and decay in ion-nonpolar molecule collisions.[15] The study was of a model of the $Cl^- + Cl_2 \rightleftarrows [Cl_3^-]^*$ systems. The potential was constructed by summing pairwise Morse functions. The purpose of the study was to carry out a preliminary investigation of the fundamental nature of the dynamics of capture and decay on a purely attractive potential-energy surface. Thus, we made no attempt to design a realistic, accurate model, but instead used one that made the calculations easy. We computed cross sections for complex formation $\bar{\sigma}_f$ as a function of lifetime and collision energy as well as decay curves for the unimolecular dissociation of the complex. We found that the $[Cl_3^-]^*$ complexes decay with random lifetimes. The capture crsss sections at a given energy are also exponentially dependent on the lifetime of the complex (as a result of the exponential decay). For convenience, we measured lifetimes of the complexes for the purpose of computing capture cross sections in terms of the number of inner turning points in the $Cl^- \cdots Cl_2$ relative motion that the complex experienced before it dissociated. The computed cross sections are exponentially dependent on the collision energy rather than having the $E^{-1/2}$ dependence predicted by the Langevin model. This is true for the total capture cross section (which includes all complexes that live for more than one inner turning point) as well as for the cross sections for forming complexes that live for a given number of inner turning points. Rate coefficients for complex formation were computed from the $\sigma(E)$. The trajectory computed value for the total capture is about 1/3 that predicted by the Langevin model.

Here we present the results of a quasiclassical tra-

jectory study of the $Cl^- + Cl_2$ system in which we have employed an empirical ion-induced-dipole plus repulsion potential. We have computed capture cross sections as a function of collision energy and complex lifetime. The distribution of complex lifetimes was computed for some cases in order to characterize the decay. We have also studied several other (model) systems in an effort to determine the effects of ion mass on complex formation (masses appropriate for H, T, Li, F, Cl, and Br were used).

Our purpose in these studies is to develop a more refined understanding of ion–molecule capture. Our trajectory results show that the collision and complex dynamics are well behaved and can be described by simple analytical forms. Such information can lead to improved understanding of termolecular ion-molecule association reactions[17] and the bigger problem of clustering of neutral molecules upon a central ion.[18] The process we study here is the first step in both of these. We have selected the $Cl^- + Cl_2$ system as the prime subject of our studies because of the experimental studies of Babcock and Streit.[19]

It should be noted that the long-range forces in ion-molecule collisions are similar to those in van der Waals systems. In general, ion–molecule bonds are stronger than those for van der Waals molecules. However, in ion-induced-dipole bonding the attraction is not always significantly greater than van der Waals attraction. The systems studied here are relatively weakly bound. The Cl_3^- complex apparently involves some covalent bonding (see Ref. 19, and references therein). Our first study involving pairwise potentials is an appropriate model for covalent interactions, while this study treats the attraction as purely electrostatic. These models are designed to investigate some general aspects of ion–molecule complex formation and dissociation rather than to represent a realistic model of a specific system.

II. COMPUTATIONAL PROCEDURES

A. Potential-energy surface

We have constructed an empirical potential that includes the r^{-4} ion-induced-dipole term used in the Langevin model. We have added to this two pairwise repulsions terms for the $Cl^- ---Cl$ short-range interactions and a Morse function to represent the Cl_2 forces. The potential has the form

$$V = Ae^{-br_1} + Ae^{-br_3} - \alpha q^2/2R^4 + D\{1 - \exp[-\beta(r_2^2 - r_e)]\}^2 ,$$
(3)

where r_1 and r_3 are the two $Cl^- ---Cl$ distances, r_2 is the Cl_2 internuclear separation, and R is the distance between Cl^- and the center of mass of Cl_2. The values of the parameters are given in Table I; q is the electronic charge. The $Cl^- ---Cl$ repulsion terms were taken to be those for $Cl^- ---Ar$ given by Spears.[20] The Cl_2 Morse potential parameters are the same as used in Ref. 15.

The same potential-energy surface was used for all the systems studied. This potential-energy surface

TABLE I. Potential parameters.

$A = 480$ eV[a]
$b = 1.37$ a.u.$^{-1}$[a]
$\alpha = 31.11$ a.u.^{3}[b]
$D = 2.51$ eV[c]
$\beta = 1.07696$ a.u.$^{-1}$[c]
$r_e = 3.757$ a.u.[c]

[a]From Spears, Ref. 20.
[b]From K. G. Denbigh, Trans. Faraday Soc. **36**, 936 (1940).
[c]From R. N. Porter, L. B. Sims, D. L. Thompson, and L. M. Raff, J. Chem. Phys. **58**, 2855 (1973).

is purely empirical. There is neither theoretical nor experimental information by which the potential can be judged (we gave a discussion and references in Ref. 15 for the sparse and relatively inaccurate results that provide information on the Cl_3^- potential). The true Cl_3^- interactions are, no doubt, poorly represented by Eq. (3). Thus, the systems examined in the present study must be viewed as models of the real ones. However, these models can provide very useful information about the fundamental nature of ion–molecule capture. Furthermore, it should be noted that simple potentials (such as the r^{-n} type) are the mainstay of ion–molecule collision theory.

B. Trajectory calculations

Trajectories were carried out to obtain: (1) the cross sections σ_f for forming complexes which live for a given number of turning points in the relative motion of the ion and center-of-mass of the molecule, and (2) σ_f^{total}, the cross section for formation of complexes which live for more than one turning point. These cross sections were computed as a function of collision energy and the mass of the ion.

Each trajectory was initiated in the ion + Cl_2 limit (where the initial separation was taken to be 15 a.u.). The trajectory was integrated until the ion and molecule center-of-mass distance reached 20 a.u. or 1.077×10^{-11} s trajectory time had elapsed. The trajectories were integrated by using a fourth-order Runge–Kutta–Gill routine with a fixed stepsize of 5.387×10^{-16} s. Integration accuracy was checked by the usual methods.[15] In all the calculations the Cl_2 molecule initially possessed only zero-point vibrational energy. The initial vibrational phase of the Cl_2 was randomly selected by using the Porter, Raff, and Miller[21] method. The maximum impact parameter was usually 14 a.u. The calculations were carried out at collision energies that are in the range of those with high probabilities at thermal equilibrium. Most of the calculations are for $E_{rel} = 0.038$ eV, the most probable collision energy at room temperature. Ensembles of 1000 to 3000 trajectories were used to compute the cross sections for each set of initial conditions.
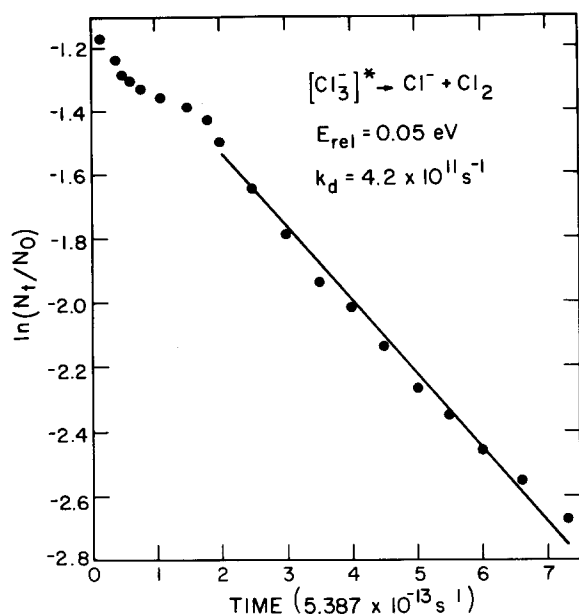
FIG. 1. Decay curve for $Cl^- + Cl_2 \rightleftarrows [Cl_3^-]^*$ with fixed energy $(E_{rel} = 0.05$ and 0.035 eV initial zero-point vibrational energy in Cl_2). Impact parameters were averaged over the range $0 \leq b \leq 14$ a.u. This plot is for an ensemble of 1000 trajectories.

Plots of lifetime distribution were made by defining the lifetime of the complex as the time that elapsed between the first and last inner turning point in the relative motion of ion and the center-of-mass of the molecule. This eliminates the time for approach and escape of the ion. Obviously, trajectories that experience only
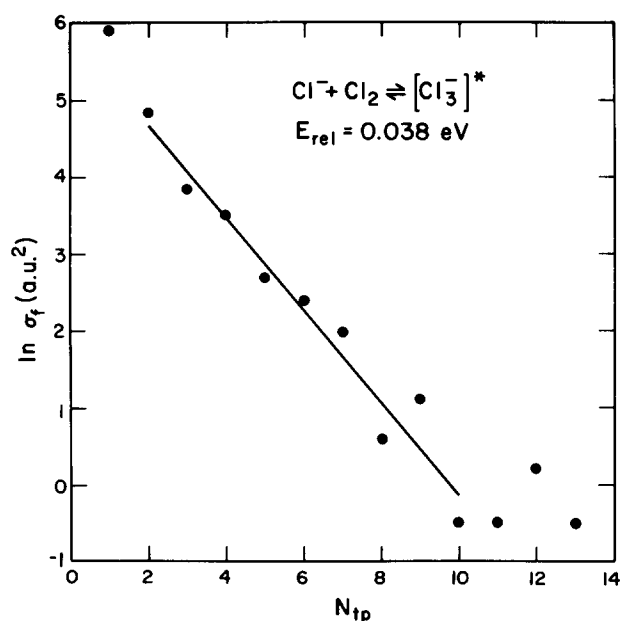

FIG. 2. Plot of the natural logarithm of the cross sections for forming a $[Cl_3^-]^*$ complex in $Cl^- + Cl_2$ collisions that lives for N_{tp} inner turning points in the $Cl^- - - -Cl_2$ relative motion as a function of N_{tp}. The results are from 1000 trajectories at $E_{rel} = 0.038$ eV (Cl_2 initially has 0.035 eV zero-point vibrational energy).
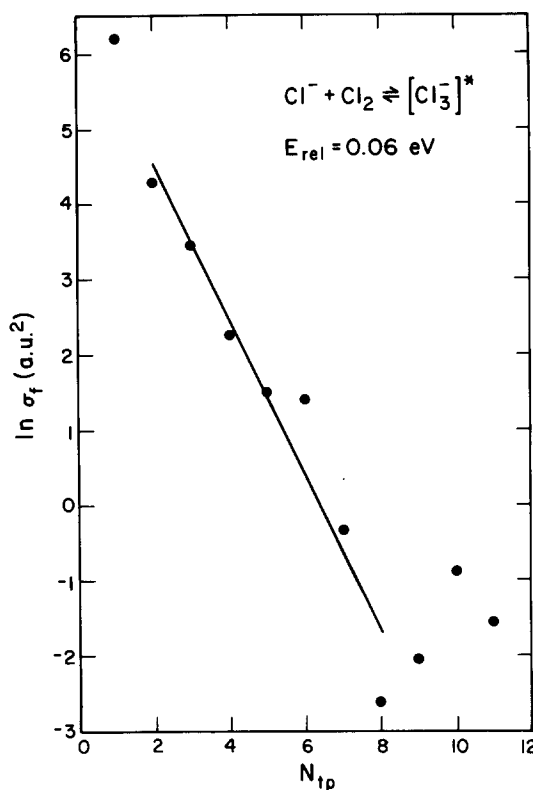

FIG. 3. Same as Fig. 2, except the results were obtained from 3000 trajectories at $E_{rel} = 0.06$ eV.

one inner turning point have zero lifetimes by this definition.

III. RESULTS AND DISCUSSION

Calculations were carried out as a function of collision energy (over the range $0.036-0.06$ eV), ion mass, and internal energy. The model studied is one based on trichloride in which we assume that Cl^- interacts with Cl_2 at long range with ion-induced dipole forces and in the short-range region with a simple exponential repulsion. The calculations to investigate the influence of the ion mass in $X^+ + Cl_2$ collisions were carried out on this Cl_3^- potential.

The ion—molecule capture process leads to the formation of an energetically unstable complex. We computed cross sections for the formation of complexes that live for given times, measured in terms of the number of inner turning points that the complex experiences before dissociation. Thus, these cross sections are dependent on the nature of the unimolecular decay process. Figure 1 shows a typical decay curve for $[Cl_3^-]^* \rightarrow Cl^- + Cl_2$. Here we have plotted the trajectory computed distribution of complex lifetimes assuming

$$\ln(N_t/N_0) = -k_d t , \qquad (4)$$

where N_t is the number of complexes that live for time t and N_0 is the total number of trajectories. As can be seen by the results in Fig. 1, the $[Cl_3^-]^*$ complexes decay exponentially. The results in Fig. 1 were obtained from an ensemble of 1000 trajectories at 0.05 eV collision energy (the total energy is the collision

TABLE II. Computed cross sections for various E_{rel} values for forming a $[Cl_3^-]^*$ complex that lives for N_{tp} inner turning points in the motion of the Cl^- relative to the Cl_2 center-of-mass. The cross sections are in a.u.^{2} units. The Monte Carlo statistical error is given for one standard deviation.

N_{tp}	E_{rel} (eV)						
	0.035	0.038	0.040	0.044	0.048	0.050	0.060
1	365.0 ± 12.3	368.2 ± 9.5	385.8 ± 12.6	417.5 ± 12.6	432.9 ± 8.9	423.6 ± 9.0	496.9 ± 7.5
2	119.3 ± 9.3	126.2 ± 7.9	109.6 ± 8.9	117.8 ± 9.2	110.2 ± 7.5	114.5 ± 7.6	73.1 ± 4.2
3	59.0 ± 7.2	46.8 ± 5.2	57.0 ± 7.1	39.8 ± 5.8	35.7 ± 4.6	40.0 ± 4.8	31.4 ± 2.9
4	30.8 ± 5.1	33.2 ± 4.4	18.6 ± 4.0	22.7 ± 4.5	16.6 ± 3.2	17.8 ± 3.3	9.6 ± 1.6
5	17.9 ± 4.0	14.8 ± 3.0	13.1 ± 3.4	7.1 ± 2.3	9.2 ± 2.4	9.2 ± 2.4	4.5 ± 1.0
6	9.3 ± 2.8	11.1 ± 2.6	12.2 ± 3.2	2.9 ± 1.2	2.5 ± 1.2	3.1 ± 1.4	4.0 ± 1.0
7	7.9 ± 2.4	7.4 ± 2.1	5.7 ± 2.3	5.4 ± 2.1	3.1 ± 1.4	3.7 ± 1.5	0.7 ± 0.4
8	7.4 ± 2.4	1.8 ± 1.0	4.9 ± 1.8	1.6 ± 0.9	1.2 ± 0.9	1.2 ± 0.9	0.1 ± 0.1
9	4.2 ± 2.0	3.1 ± 1.4	2.2 ± 1.3	$\cdots$	1.8 ± 1.1	$\cdots$	0.1 ± 0.1
10	0.8 ± 0.8	0.6 ± 0.6	1.0 ± 0.7	$\cdots$	$\cdots$	$\cdots$	0.4 ± 0.3
11	0.8 ± 0.8	0.6 ± 0.6	1.6 ± 1.1	$\cdots$	$\cdots$	$\cdots$	0.2 ± 0.2
12	2.4 ± 1.4	1.2 ± 0.9	$\cdots$	0.7 ± 0.7	$\cdots$	$\cdots$	$\cdots$
13	0.3 ± 0.3	0.6 ± 0.6	$\cdots$	0.7 ± 0.7	$\cdots$	$\cdots$	$\cdots$
14	$\cdots$	$\cdots$	$\cdots$	$\cdots$	$\cdots$	$\cdots$	0.2 ± 0.2
15	0.6 ± 0.6	$\cdots$	0.2 ± 0.2	$\cdots$	$\cdots$	$\cdots$	$\cdots$

energy plus 0.035 eV zero-point energy). The impact parameters for the formation collisions were Monte Carlo selected over the range $0 \le b \le 14$ a.u. We have shown in previous work[15] as well as in the present case
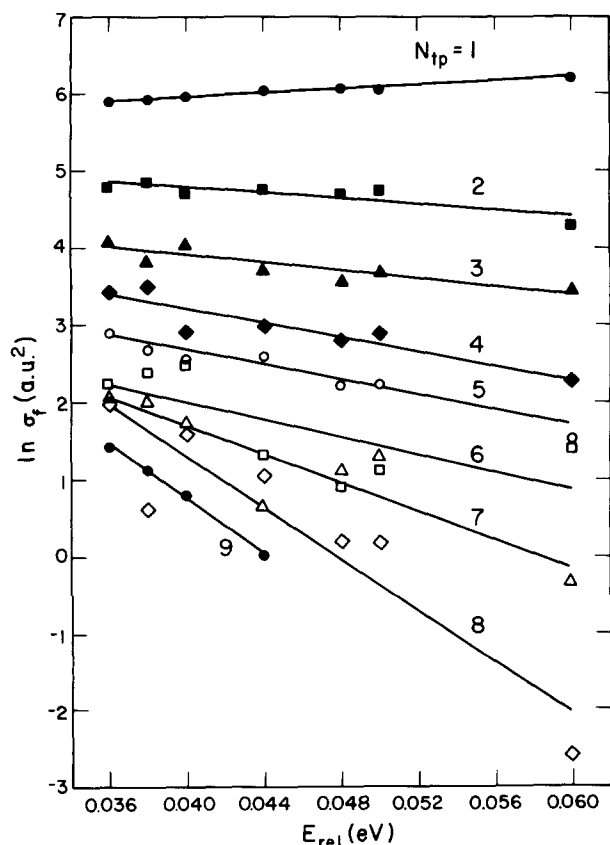

FIG. 4. Plots of the natural logarithm of the cross sections for forming $[Cl_3^-]^*$ complexes, in $Cl^- + Cl_2$ collisions, that live for 1, 2, ..., 9 inner turning points in the $Cl^- - - -Cl_2$ relative motion as a function of the initial relative translational energy. The solid lines are least-squares fits of the points.

that the angular momentum can be averaged over without discernable influence on the fit of the trajectory results to Eq. (4). The negative of the slope of the decay curve is the unimolecular dissociation rate constant $k_d(E)$, which for the conditions plotted in Fig. 1 is 4.2 $\times 10^{11}$ s^{-1}.

The cross sections σ_f for forming complexes that live for a given number N_{tp} of inner turning points in the $Cl^- - - -Cl_2$ relative motion, were computed for a range of initial conditions. The cross sections σ_f obey

$$\sigma_f = \sigma_0 e^{-mN_{tp}}, \tag{5}$$

as shown by the plots in Figs. 2 and 3 for $E_{rel} = 0.038$ and 0.06 eV, respectively. These results are typical of those obtained for $Cl^- + Cl_2 \rightleftharpoons [Cl_3^-]^*$ over the energy range studied. The results in Fig. 2 were obtained from an ensemble of 1000 trajectories and those in Fig. 3 from 3000 trajectories. The solid lines in the figures are least-squares fits of the results to Eq. (5) for the range over which the line extends. In fitting the points, we ignored the $N_{tp} = 1$ values because they do not represent complex formation. The points for large N_{tp} values were ignored because of the high statistical error in them.

Table II gives the computed values of σ as a function of N_{tp} for $E_{rel} = 0.036$, 0.038, 0.04, 0.044, 0.048, 0.05, and 0.06 eV. As the energy increases, the magnitudes of the cross section for forming a complex that lives for several N_{tp} decreases. That is, the rate of decay of the complex increases as the energy increases. The cross section for forming a complex that lives for $N_{tp} = 2$ is much less energy dependent. The least-squares fits give $\sigma_0 = 354.2$ a.u.^{2}, $m = -0.60$, and $\sigma_0 = 765.1$ a.u.^{2}, $m = -1.04$ for $E_{rel} = 0.038$ (Fig. 3) and 0.060 eV (Fig. 4), respectively.

The formation cross section σ_f depends exponentially on the collision energy as illustrated by the plots of the natural logarithms of σ_f against E_{rel} for $N_{tp} = 1$ through 9 shown in Fig. 4. The solid lines in Fig. 4 were ob-

TABLE III. Comparison of the intercepts (a) and slopes (b) for the results shown in Fig. 4 and the bimolecular rate coefficients computed from these using Eq. (7) for complexes that live 1, 2, ..., 9 inner turning points.

N_{tp}	a (a.u.^{2})	b(eV^{-1})	k(cm^3/molecule s)
1	225.9	−13.2	7.6×10^{-10}
2	249.6	18.5	1.6×10^{-10}
3	134.3	24.9	7.2×10^{-11}
4	154.5	45.9	4.7×10^{-11}
5	120.3	53.4	3.1×10^{-11}
6	68.0	55.9	1.6×10^{-11}
7	221.4	92.6	2.8×10^{-11}
8	2951.3	167.4	1.5×10^{-10}
9	2540.2	177.1	1.2×10^{-10}

tained by least-squares fits of the results to

$$\sigma_f = a e^{-bE_{rel}} . \tag{6}$$

The values of the parameters a and b for the various N_{tp} are given in Table III. Also given in the last column of Table III are values of the rate coefficient at 300 K computed from

$$k(T) = (\Pi\mu)^{-1/2} (2/\kappa T)^{3/2} a(b + 1/\kappa T)^{-2} , \tag{7}$$

which is obtained by integrating Eq. (6) over the Boltzmann distribution of relative translational energies. There is considerable scatter, due to statistical error (see the results in Table II), in the cross section values for the larger N_{tp} values. Thus, the results given in Table III for these large N_{tp} values are only qualitatively accurate at best. It is clear, however, that the slopes of the lines in Fig. 4 increase significantly as N_{tp} increases. The unimolecular rate coefficient values (given in the last column of Table III) decrease as N_{tp} increases; the fact that the values for $N_{tp} = 8$ and 9 do not fit this trend is probably due to statistical error. The values for the ion-induced-dipole potential (Table III) are comparable in magnitude to those for the Morse-function potential used in our previous study (see Table II of Ref. 15).

Figure 5 shows a plot of the natural logarithm of the cross section for forming complexes that live for more than one inner turning point in the $Cl^- $---$Cl_2$ relative motion as a function of the initial relative translational energy. These values also obey Eq. (6); the solid line is a least-squares fit. The values of parameters in Eq. (6) obtained by the fitting are $a = 742.5$ a.u.^{2} and $b = 29.3$ eV^{-1}. Using these in Eq. (7), we obtain 3.5×10^{-10} cm^3/molecule s for the bimolecular rate coefficient at 300 K. This value is essentially the same as that obtained in our previous study[15] in which we obtained $k = 3.2 \times 10^{-10}$ cm^3/molecule s at 300 K. This is interesting because the two potentials are significantly different. The values of the parameters for Eq. (6) obtained in the earlier study, in which we used a potential with a much deeper well than here, are $a = 254.7$ a.u.^{2} and $b = 2.7$ eV^{-1}. The energy dependence is much greater for the ion-induced-dipole potential used here than for the Morse potential used in the previous study.[15] Thus, it is a coincidence that the rate coefficients for the two

potentials have the same value. It results, no doubt, from the balancing of the ease of forming a complex in the case of the deeper well and the influence of the long-range attraction of the ion-induced-dipole potential on complex formation. It should be noted that probably neither potential is appropriate for the real $Cl^- + Cl_2$ system. The real system probably involves covalent bonding and most certainly involves long-range attraction due to ion-induced-dipole forces.

Although a direct comparison is not appropriate, since different definitions of capture are used, it is interesting to note that our trajectory result for the capture rate constant is 30 times smaller than that predicted by the Langevin theory. The Langevin rate coefficient is given by

$$k_L = 2\pi q (\alpha/\mu)^{1/2} . \tag{8}$$

If we use $\alpha = 46.1 \times 10^{-25}$ cm^3 for the polarizability, we obtain $k_L = 1.03 \times 10^{-9}$ cm^3/molecule s.

We investigated the influence of Cl_2 initial vibrational and rotational excitation on $[Cl_3]^*$ complex formation at 0.05 eV initial relative translational energy. The cross sections for forming complexes that live N_{tp} inner turning points for Cl_2 initially in the ground v, J states at $E_{rel} = 0.05$ eV are given in the next to last column of Table II. The results for various initial Cl_2 excitations are compared in Table IV. The first column of Table IV gives the initial v, J values for Cl_2. The next four columns list the ratios of the cross sections for forming a complex that lives $N_{tp} = 2$, 3, 4, and 5 inner turning-points for $\sigma_f (v = 0, J = 0)/\sigma_f (v, J)$. The sixth column gives the total cross section for forming complexes that live for $N_{tp} > 1$. The last two columns are the values of the parameters in Eq. (5) obtained by least-squares fitting.

In all cases, initial Cl_2 excitation decreases the cross section for complex formation, but not dramatically, considering the amounts of energy involved. Initial rotation appears to have the greater effect on the results. The total complex formation cross section drops
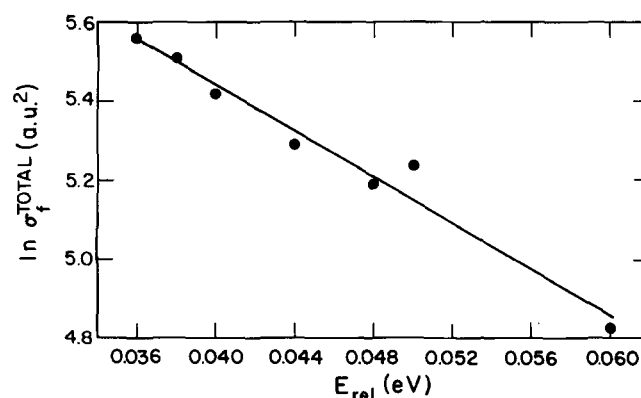

FIG. 5. Plot of the natural logarithm of the cross section for forming a $[Cl_3]^*$ complex, in a $Cl^- + Cl_2$ collision, that lives for two or more inner turning points in the $Cl^- $---$Cl_2$ relative motion as a function of the initial relative translational energy. The solid line is a least-squares fit of the points.

TABLE IV. Influence of Cl_2 initial excitation on complex formation cross sections at $E_{rel} = 0.05$ eV. The values given are the ratios of cross section values for $v = 0$, $J = 0$ to those for the specified v, J values. Also given are the values of the parameters for Eq. (5) obtained by least-squares fitting.

| | N_{tp} | | | | Total | | |
v, J	2	3	4	5	σ_f (a. u.^{2})	σ_0 (a. u.^{2})	m
0, 0	1	1	1	1	188.4 ± 10.9	550.0	0.84
0, 10	1.24	1.14	1.29	1.82	160.8 ± 10.4	645.5	0.97
0, 20	1.65	1.32	1.36	0.58	142.5 ± 9.7	368.7	0.84
1, 0	1.41	1.05	1.24	2.42	147.3 ± 10.0	727.8	1.02
2, 0	1.28	1.18	1.14	1.67	151.0 ± 10.2	523.2	0.90

from 188 to 142 a. u. when J is increased from zero to 20, an increase of about 1×10^{-2} eV in energy. The change in total cross section is less than this for a change of $v = 0$ to $v = 2$ in vibrational state, which involves an increase of about 0.14 eV in internal energy. But the influence of internal energy is relatively minor. This is further illustrated by the plots shown in Fig. 6, in which the results for $v = 0$ and $v = 2$ are compared. The $v = 0$ results are represented by the solid line (least-squares fit) and circle while those for $v = 2$ are represented by the dashed line and squares.

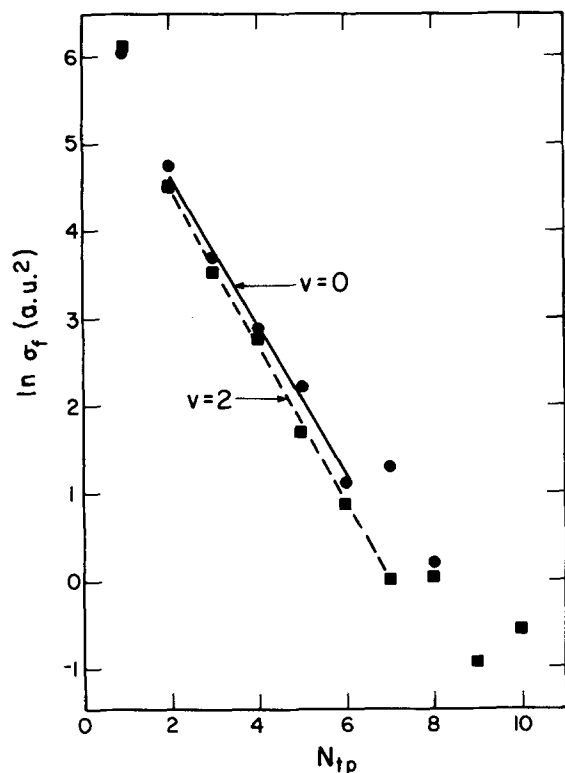We have also studied complex formation as a function

of ion mass. In these calculations we used the model Cl_3^- potential. All the calculations are for $E_{rel} = 0.038$ eV and Cl_2 in the ground vibrational-rotational states (the Cl_2 zero-point vibrational energy is 0.035 eV). Masses appropriate for hydrogen, tritium, lithium, fluorine, chlorine, and bromine were considered. In all the cases except Cl^-, 2000 trajectories were computed to obtain the formation cross sections as a function of the number of inner turning points.

Typical results are illustrated by the cases of "Li^+" and "F^-" + Cl_2 in Figs. 7 and 8, respectively. The solid lines in these figures are obtained by least-squares fitting of the results to Eq. (5).

These two plots illustrate a trend observed in the ion mass dependence of the complex formation—a greater tendency as the mass decreases to form complexes that live for many N_{tp}. In the cases of ion masses 1.0 and 3.0 amu, complexes were formed which lived for more than 30 inner turning points. The cross sections for forming these long-lived complexes are quite small, however. For example, the cross section for forming
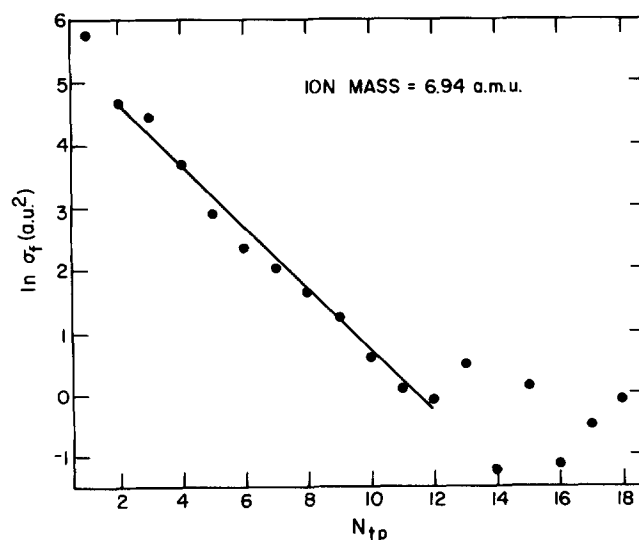

FIG. 6. Plots of the natural logarithm of the cross section for forming a $[Cl_3^-]^*$ complex that lives for N_{tp} inner turning points in the Cl^- - - - Cl_2 relative motion as functions of N_{tp}. The circles and solid line are for Cl_2 initially in the ground-vibrational state and the squares and dashed line are for Cl_2 in the second excited vibrational state. In both cases, there is initially no Cl_2 rotational energy. The lines are least-squares fits of the points.

FIG. 7. Plot of the natural logarithm of the cross sections for forming a complex, in collisions between Cl_2 and an ion of mass 6.94 amu on the Cl_3^- potential-energy surface, that lives for N_{tp} inner turning points in the relative motion of the ion and molecule as a function of N_{tp}. The results are for 2000 trajectories at $E_{rel} = 0.038$ eV (Cl_2 initially has 0.035 eV zero-point vibrational energy).

TABLE V. Comparison of complex formation for various ion masses.[a]

Ion mass (amu)	σ_f (a. u.^{2})[b]	m[b]	σ_f^{Total} (a.u.^{2})
1.0	148.4	1.0	37.0 ± 3.1
3.0	487.8	0.8	184.6 ± 7.7
6.94	273.1	0.49	287.5 ± 9.0
19.0	445.8	0.63	281.8 ± 9.2
35.45	354.2	0.60	246.4
79.91	379.9	0.76	155.4 ± 7.5

[a]$E_{\text{rel}} = 0.038$ eV. Initial Cl_2 vibrational energy equals 0.035 eV.
[b]Values obtained by least-squares fitting of trajectory results to Eq. (5).

all the complexes which live for $N_{tp} > 20$ is only 1.6 a.u.^{2} in the case of tritium ion mass, and only 0.4 a.u.^{2} for the hydrogen case. One would expect, of course, simply on the basis of mass that at a given energy the lighter the ion, the greater the number of vibrations that it can undergo in a given time.

The results for all the masses studied are summarized in Table V. The mass of the ion is given in the first column, the next two columns give the values of parameters for Eq. (5) that were obtained by least-squares fittings, and the last column gives the cross section for forming all complexes that live for more than one inner turning point. The parameter m is the negative of the slopes of the plots such as shown in Figs. 7 and 8. The value of m is greatest for mass 1.0 amu. It decreases from unity for hydrogen to 0.49 for lithium, then levels off (more or less) for the larger masses (the value of
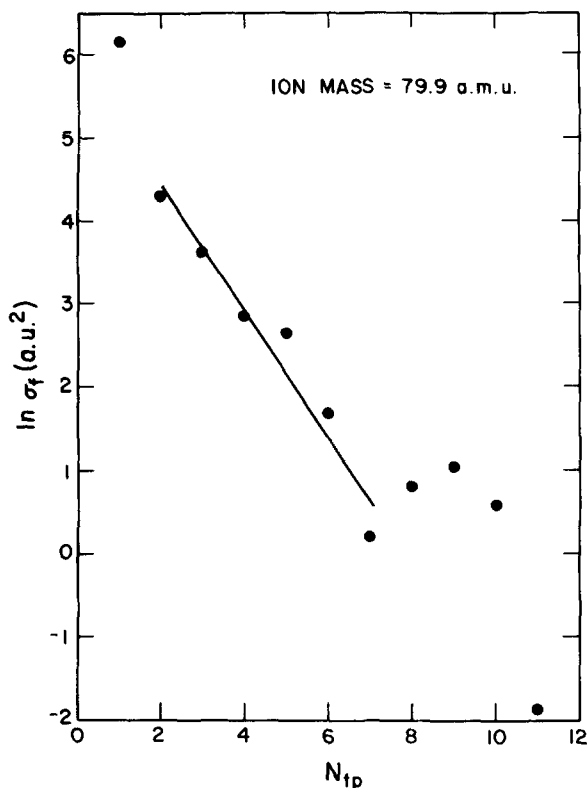

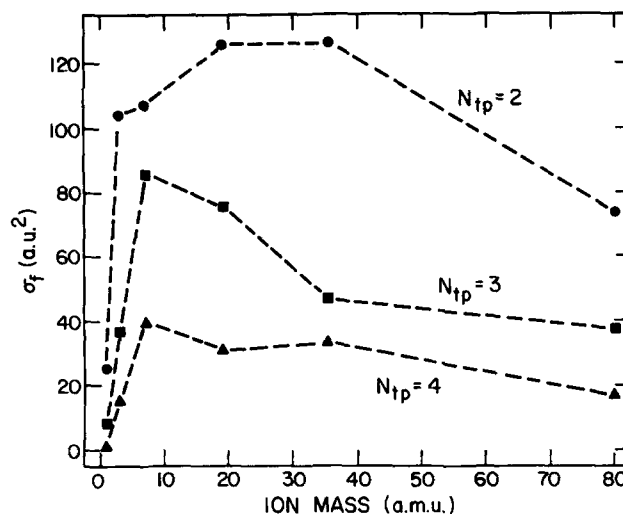FIG. 8. Same as Fig. 7, except ion mass equals 79.9 amu.

FIG. 9. Plots of the cross sections for forming complexes that live for 2, 3, and 4 inner turning points in the motion of the ion relative to the Cl_2 center-of-mass as functions of the ion mass. The results were obtained by using the Cl_3^- potential. The relative translational energy is 0.038 eV and Cl_2 initially possesses zero-point vibrational energy (0.035 eV).

m for the bromide ion is significantly larger, thus there may be a gradual increase in m from F$^-$ and up rather than a leveling off). A related trend is seen in the values for the total complex-formation cross section σ_f^{total} given in the last column of Table V. It goes through a maximum at the mass of the lithium ion. The increase in σ_f^{total} is more abrupt than is the falloff. Similar behavior is found for the cross sections for forming a complex that lives for a given number of inner turning points. Figure 9 shows plots of the cross sections, as a function of ion mass, for forming complexes that live for 2, 3, and 4 inner turning points. Again, as the ion mass increases there is a sharp increase, then a gradual falloff. For $N_{tp} = 2$, the maximum occurs in the region of the F$^-$ and Cl$^-$ masses.

IV. SUMMARY

We have used quasiclassical trajectories to investigate ion–molecule capture for a potential that is exponential at short range and ion-induced-dipole r^{-4} at long range. The potential model is based on Cl$^-$+Cl$_2$ and most of the calculations are for this system. However, we also investigated the influence of ion mass using this same potential.

The purpose of these model studies was to investigate ion–molecule capture and complex lifetime for a purely electrostatic model of the long-range attraction. In a previous study,[15] we investigated the Cl$^-$+Cl$_2 \rightleftharpoons$ [Cl$_3^-$]* system using a potential that is a more appropriate model of a system with covalent bonding.

We have computed cross sections for forming ion–molecule complexes as a function of the complex lifetime (measured in terms of the number of inner turning points in the motion of the ion relative to the center-of-mass of Cl$_2$. Although the emphasis of the study is on the calculations of formation cross sections, we also

examined the nature of the unimolecular decay of the complexes. The unimolecular dissociation occurs with random lifetimes. Both the decay curves and the lifetime-dependent formation cross sections are well described by single exponentials.

The calculations were carried out on fixed values of the relative translational energy over the range 0.036 to 0.06 eV. In most of the calculations the Cl_2 initially possessed only zero-point vibrational energy. An investigation of the influence of initial Cl_2 vibrational and rotational excitation revealed only slight variation in the results for $J = 0$, 10, and 20 and for $v = 0$, 1, and 2. Thermal rate coefficients were computed for $Cl^- + Cl_2 \rightarrow [Cl_3^-]^*$ by averaging the cross sections over the Boltzmann distribution of relative velocities. We obtained a value at 300 K that is in close accord with the value computed in our earlier study.[15] Since the potentials are drastically different we must assume that this is fortuitous.

The influence of the ion mass was found to be quite strong for masses up to that for lithium (sharp increase in complex formation) but relatively weak for masses between 19 and 79.9 amu (gradual decrease in complex formation).

[1] G. Gioumousis and D. P. Stevenson, J. Chem. Phys. 29, 294 (1958).

[2] See, for example, M. Henchman, in *Ion–Molecule Reactions*, edited by J. L. Franklin (Plenum, New York, 1972), Vol. 7, p. 101.

[3] J. V. Dugan, Jr., and J. I. Magee, J. Chem. Phys. 47, 3103 (1967).

[4] J. V. Dugan, Jr., J. H. Rice, and J. L. Magee, Chem. Phys. Lett. 3, 323 (1969).

[5] J. V. Dugan, Jr., R. W. Palmer, and J. L. Magee, Chem. Phys. Lett. 6, 158 (1970).

[6] J. V. Dugan, Jr., Chem. Phys. Lett. 8, 198 (1971).

[7] J. V. Dugan, Jr., and R. B. Canright, Jr., Chem. Phys. Lett. 8, 253 (1971).

[8] J. V. Dugan, Jr. and R. W. Palmer, Chem. Phys. Lett. 13, 144 (1972).

[9] J. V. Dugan, Jr. and R. B. Canright, Jr., J. Chem. Phys. 56, 3623 (1972).

[10] J. V. Dugan, Jr. and J. L. Magee, J. Chem. Phys. 58, 5816 (1973).

[11] W. J. Chesnavich, T. Su, and M. T. Bowers, J. Chem. Phys. 72, 2641 (1980).

[12] T. Su and W. J. Chesnavich, J. Chem. Phys. 76, 5183 (1982).

[13] W. L. Hase and D.-F. Feng, J. Chem. Phys. 75, 738 (1981).

[14] K. N. Swamy and W. L. Hase, J. Chem. Phys. 77, 3011 (1982).

[15] L. M. Babcock and D. L. Thompson, J. Chem. Phys. 78, 2394 (1983).

[16] J. B. Anderson, J. Chem. Phys. 58, 4684 (1973).

[17] For a recent review of termolecular ion–molecule reactions, see D. Smith and N. G. Adams, in *Gas Phase Ion Chemistry*, edited by M. T. Bowers (Academic, New York, 1979), Vol. I, p. 1.

[18] For a recent review of ion–molecule nucleation, see A. W. Castleman, Jr., in *Kinetics of Ion–Molecule Reactions*, edited by P. Ausloos (Plenum, New York, 1979), p. 295.

[19] L. M. Babcock and G. E. Streit, J. Chem. Phys. 76, 2407 (1982).

[20] K. G. Spears, J. Chem. Phys. 57, 1842 (1972).

[21] R. N. Porter, L. M. Raff, and W. H. Miller, J. Chem. Phys. 63, 2214 (1975).